RADIATIVE MAGNETOHYDRODYNAMIC COMPRESSIBLE COUETTE FLOW IN A PARALLEL CHANNEL WITH A NATURALLY PERMEABLE WALL

by

Paresh VYAS[a]* and Nupur SRIVASTAVA[b]

[a] Department of Mathematics, University of Rajasthan, Jaipur, India
[b] Department of Mathematics, Swami Keshvanand Institute of Technology, Management and Gramothan, Jaipur, India

Original scientific paper
DOI: 10.2298/TSCI120828099V

The paper pertains to investigations of thermal radiation effects on dissipative magnetohydrodynamic Couette flow of a viscous compressible Newtonian heat-generating fluid in a parallel plate channel whose one wall is stationary and naturally permeable. Saffman' slip condition is used at the clear fluid-porous interface. The fluid is considered to be optically thick and the radiative heat flux in the energy equation is assumed to follow Rosseland approximation. The momentum and energy equations have closed form solutions. The effects of various parameters on thermal regime are analyzed through graphs and tables.

Key words: *Couette flow, magnetohydrodynamics, radiation, compressible fluid, dissipation*

Introduction

Couette flow in parallel plate channel has been a classical problem in fluid mechanics. Owing to rather simple configuration of shear flow between infinite parallel plates, and most importantly, its varied applications in diverse areas such as geothermal systems, astrophysics, industrial technologies to name a few, have prompted investigators to revisit the problem with variety of assumptions [1-5].

Flow in the presence of naturally permeable boundary is abundant in nature since most of the natural channels involve naturally permeable beds such as gravel bed rivers. Couette flow in channel with naturally permeable boundary is a fascinating situation since it models many configurations of importance, these include granular media filtration, oil recovery, mass transfer in packed-beds, groundwater hydrology, petroleum reservoir engineering, and many other. Berman [6] was probably the first to examine the laminar flow in a channel with a porous wall. Substantial work has been reported on the suitable boundary conditions at clear fluid-porous interface [7-12].

Experimentation pertaining to flow in a parallel plate channel, one of whose walls is naturally permeable layer revealed velocity slip at the porous wall [7]. This led to conclude that the shear effects are propagated into the porous strata through a boundary layer region and the effect can be summarized as a slip condition at the fluid-porous medium boundary. It is pertinent to record that the no slip boundary condition for velocity at the wall is strictly valid only for viscous flows in contact with solid, impermeable surfaces. The “Klinkenberg" effect [13] *i. e.* seepage occurring during the motion of gases in porous media is an outcome of

* Corresponding author; e-mail: pvyasmaths@yahoo.com

molecular effects when the mean free path of the gas molecules is comparable to or less than the length dimension of the pores.

The slug flow in the permeable bed is governed by Darcy's law, but it is pertinent to note that in the absence of any external pressure gradient and for small permeability, the interior flow of the porous medium would not contribute much to the exterior clear fluid flow, and, therefore, zero-filter velocity in the permeable bed may be assumed [3]. However, the permeability of the lower bed affects the clear fluid flow through the slip condition as suggested by Saffman [14] who showed that for small permeability, the following equation is appropriate to compute the exterior clear fluid flow correct to o(k):

$$u = \frac{\sqrt{k}}{\alpha}\left(\frac{\partial u}{\partial y}\right)_{y=0^+} + \mathrm{o}(k)$$

where u is the fluid velocity, k – the permeability, and α – the empirical constant depending upon the porous medium. Studies pertaining to configurations having permeable lining which may have low permeability values are of interest in designing engineering equipment. Magnetohydrodynamic (MHD) flow in porous media or permeable beds has been studied extensively because it plays a vital role in the performance of many systems in industry [17].

Heat transfer in a radiating fluid with slug flow in a parallel plate channel was investigated by Viskanta [18] who formulated the problem in terms of integro-differential equations and solved by an approximate method. Helliwell [19] discussed the stability of thermally radiative magnetofluiddynamic channel flow. Elsayed *et al*. [20] provided numerical solution for simultaneous forced convection and radiation in parallel plate channel and presented analysis for the case of non-emitting "blackened" fluid. Helliwell *et al*. [21] discussed the radiative heat transfer in horizontal magnetohydrodynamic channel flow considering the buoyancy effects and an axial temperature gradient. Elbashbeshy *et al*. [22] studied heat transfer over an unsteady stretching surface embedded in a porous medium in the presence of thermal radiation and heat source or sink. The viscous heating aspects in fluids were investigated for its practical interest in polymer industry and the problem was invoked to explain some rheological behavior of silicate melts. The importance of viscous heating has been demonstrated by Gebhart [23], Gebhart *et al*. [24], Magyari *et al*. [25], and Rees *et al*. [26].

The Couette flow studies pertaining to compressible fluid are scanty. Illingworth [27] presented some exact solutions of the Navier-Stokes equations of a viscous compressible fluid and found that only solutions similar to Couette flows of an incompressible fluid are obtained in simple closed form. A further extension to Couette flow for compressible fluid was given by Morgan [28]. This paper investigates the thermal radiation effects on dissipative MHD Couette flow of a viscous compressible Newtonian heat-generating fluid in a parallel plate channel with a naturally permeable wall for two cases-isothermal walls and adiabatic-isothermal walls. It is expected that the present work would serve as a pertinent preliminary model to peep into real analogous systems.

Mathematical formulation

Let us consider laminar radiative MHD Couette flow of a viscous compressible absorbing-emitting but non-scattering optically thick Newtonian heat-generating fluid in a parallel plate channel. The lower wall is a stationary naturally permeable boundary maintained at uniform temperature T_0 while the upper plate is an impermeable plane moving with constant velocity u_1. Two cases have been considered here; *Case I*: both the plates bear different uniform temperatures T_0 and T_1, and *Case II*: isothermal lower wall and adiabatic upper wall.

A Cartesian co-ordinate system is used as shown in the schematic diagram (fig. 1). The pressure at the origin is p_0. The set-up is exposed to a transverse magnetic field of strength B_0 which is fixed relative to the fluid. The induced magnetic field is neglected, which is valid for small magnetic Reynolds number and furthermore, the electric field is zero simply because no applied or polarization voltages exist.

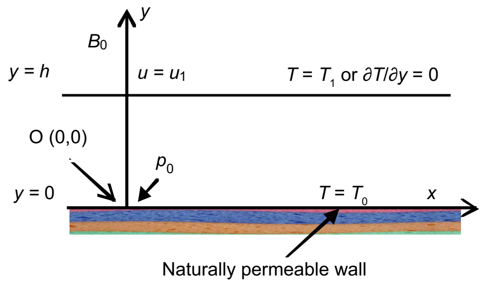

Figure 1. Schematic diagram – mathematical model

All the physical quantities except the density and the pressure are considered to be constant and it is assumed that the fluid is such that the pressure shares a functional relationship with density ρ and temperature T. Hence:

$$p = p(\rho, T) \tag{1}$$

Rosseland diffusion approximation [29], is followed to describe the radiative heat flux q_r in the energy equation and it is:

$$q_r = -\frac{4\sigma_1}{3k_1}\frac{\partial T^4}{\partial y} \tag{2}$$

where σ_1 and k_1 are Stephan-Boltzmann constant and mean absorption constant, respectively.

Here it is pertinent to mention that Rosseland approximation simulates radiation in optically thick fluids reasonably well in which thermal radiation travels short distance before being scattered or absorbed. Thus the governing equations for the set up considered are:

$$\frac{\partial \rho}{\partial x} = 0 \tag{3}$$

$$-\frac{\partial p}{\partial x} + \mu\frac{\mathrm{d}^2 u}{\mathrm{d}y^2} - \sigma B_0^2 u = 0 \tag{4}$$

$$-\frac{\partial p}{\partial y} - \rho g = 0 \tag{5}$$

$$-\frac{\partial p}{\partial z} = 0 \tag{6}$$

$$\kappa\frac{\mathrm{d}^2 T}{\mathrm{d}y^2} + \mu\left(\frac{\mathrm{d}u}{\mathrm{d}y}\right)^2 + Q_0(T - T_0) - \frac{\partial q_r}{\partial y} + \sigma B_0^2 u^2 = 0 \tag{7}$$

Together with the following appropriate boundary conditions:

$$\begin{aligned} &y = 0: \quad u = \frac{k^{1/2}}{\alpha}\frac{\partial u}{\partial y}, \quad v = w = 0, \quad T = T_0 \\ &y = h: \quad u = u_1, \qquad v = w = 0 \quad \text{case I:} \quad T = T_1 \quad \text{or} \quad \text{case II:}\ \partial T/\partial y = 0. \end{aligned} \tag{8}$$

and of the origin, *i. e.* at $x = y = z = 0$: $-\tau_{22} = p_0$.

In eq. (8) u, v, w are the velocity of the fluid, σ – the electrical conductivity, μ – the coefficient of viscosity, k – the permeability, g – the gravitational acceleration, κ – the thermal conductivity, and Q_0 – the uniform heat source.

In view of eq. (3), ρ is independent of x, hence we may take it as a function of y and z only. Further eqs. (5) and (6) indicate that density is independent of z:

$$\rho = \rho\,(y) \tag{9}$$

From eqs. (3)-(6) we find:

$$p = -\mathrm{g}\int_0^y \rho \mathrm{d}y + c_1 x + c_2 \tag{10}$$

$$u = c_3 \exp\left(\sqrt{\frac{\sigma}{\mu}} B_0 y\right) + c_4 \exp\left(-\sqrt{\frac{\sigma}{\mu}} B_0 y\right) - \frac{c_1}{\sigma B_0^2} \tag{11}$$

where c_1, c_2, c_3, and c_4 are constants of integration to be determined. Using eq. (8) we find:

$$c_2 = p_0 \tag{12}$$

In view of the eqs. (1) and (9), and noting the fact that T is a function of y only, one finds that:

$$c_1 = 0 \tag{13}$$

Thus eq. (11) reduces to:

$$u = c_3 \exp\left(\sqrt{\frac{\sigma}{\mu}} B_0 y\right) + c_4 \exp\left(-\sqrt{\frac{\sigma}{\mu}} B_0 y\right) \tag{14}$$

We now introduce the following non-dimensional quantities:

$$\begin{gathered} x^* = \frac{x}{h}, \quad y^* = \frac{y}{h}, \quad z^* = \frac{z}{h}, \quad u^* = \frac{u}{u_1}, \quad v^* = \frac{v}{u_1}, \quad w^* = \frac{w}{u_1}, \\ k^* = \frac{k}{h^2}, \quad B = \frac{\alpha h}{\sqrt{k}} = \frac{\alpha}{\sqrt{k^*}}, \quad \text{case I: } \theta = \frac{T - T_0}{T_1 - T_0} \quad \text{or} \quad \text{case II: } \theta = \frac{T - T_0}{T_0} \end{gathered} \tag{15}$$

where θ is the dimensionless temperature.

Equation (14) in non-dimensional form after dropping asterisks for convenience, becomes:

$$u = D_1 \mathrm{e}^{\mathrm{M}y} + D_2 \mathrm{e}^{-\mathrm{M}y} \tag{16}$$

where $D_1 = c_3/u_1$, $D_2 = c_4/u_1$, and M = [(σ]/μ $\mathrm{M} = (\sigma B_0^2 h^2/\mu)^{-1/2}$ is the Hartmann number. The boundary conditions (8) in non-dimensional form are obtained:

$$\begin{aligned} y=0:&\quad u=\frac{1}{B}\frac{\mathrm{d}u}{\mathrm{d}y}, \quad v=w=0, \quad \theta=0 \\ y=1:&\quad u=1, \quad v=w=0, \ \text{case I}: \theta=1 \quad \text{or} \quad \text{case II}: \frac{\mathrm{d}\theta}{\mathrm{d}y}=0 \end{aligned} \tag{17}$$

The constants D_1 and D_2 appearing in eq. (16) are evaluated in view of eq. (18) as:

$$D_1 = \frac{-\left(1+\dfrac{\mathrm{M}}{B}\right)}{\left(1-\dfrac{\mathrm{M}}{B}\right)\mathrm{e}^{-\mathrm{M}} - \left(1+\dfrac{\mathrm{M}}{B}\right)\mathrm{e}^{\mathrm{M}}} \quad \text{and} \quad D_2 = \frac{1-\dfrac{\mathrm{M}}{B}}{\left(1-\dfrac{\mathrm{M}}{B}\right)\mathrm{e}^{-\mathrm{M}} - \left(1+\dfrac{\mathrm{M}}{B}\right)\mathrm{e}^{\mathrm{M}}} \tag{18}$$

Equation (16) together with constants given by eq. (18) provides the velocity in non-dimensional form.

Having determined the velocity field we now proceed to find the temperature field for which we consider both the cases separately. We assume that the temperature difference within the fluid is sufficiently small so that T^4 may be expressed as a linear function of temperature T. This is done by expanding T^4 in a Taylor series about T_0 and omitting higher order terms to yield:

$$\begin{aligned} T^4 &= T_0^4 + 4(T-T_0)T_0^3 + 6(T-T_0)^2 T_0^2 + ... \\ T^4 &\cong 4\, T_0^3 T - 3T_0^4 \end{aligned} \tag{19}$$

Case I – Isothermal walls

The energy eq. (7) in non-dimensional form after dropping asterisks and using eqs. (2) and (19) becomes:

$$\frac{\mathrm{d}^2\theta}{\mathrm{d}y^2} + \frac{Q}{1+\dfrac{4N}{3}}\theta = \frac{-\mathrm{Br}}{1+\dfrac{4N}{3}}\left[\left(\frac{\mathrm{d}u}{\mathrm{d}y}\right)^2 + \mathrm{M}^2 u^2\right] \tag{20}$$

where $N = 4\sigma_1 T_0^3/k_1\kappa$, $\mathrm{Br} = \mu u_1^2/\kappa(T_1 - T_0)$, and $Q = Q_0 h^2/\kappa$ are the radiation parameter, Brinkman number, and heat source parameter, respectively.

Using eq. (16), eq. (20) takes the following form:

$$\frac{\mathrm{d}^2\theta}{\mathrm{d}y^2} + \frac{Q}{1+\dfrac{4N}{3}}\theta = \frac{-2\mathrm{Br}\mathrm{M}^2}{1+\dfrac{4N}{3}}(D_1^2\,\mathrm{e}^{2\mathrm{M}y} + D_2^2\,\mathrm{e}^{-2\mathrm{M}y}) \tag{21}$$

Solving eq. (21) we get the temperature as:

$$\theta = D_3\cos\tau y + D_4\sin\tau y - \frac{2\mathrm{Br}\mathrm{M}^2 N_1}{4\mathrm{M}^2 + QN_1}(D_1^2\,\mathrm{e}^{2\mathrm{M}y} + D_2^2\,\mathrm{e}^{-2\mathrm{M}y}) \tag{22}$$

where D_3 and D_4 are constants of integration and we assume that $\tau = (QN_1)^{1/2}$, and $N_1 = 1/(1 + 4N/3)$.

On applying boundary conditions (17) (for case I) to eq. (22) the constants D_3, and D_4 are obtained as:

$$D_3 = \frac{2\mathrm{BrM}^2 N_1 (D_1^2 + D_2^2)}{4\mathrm{M}^2 + QN_1}$$

$$D_4 = \frac{1}{\sin\tau}\left\{1 + \frac{2\mathrm{BrM}^2 N_1}{4\mathrm{M}^2 + QN_1}[D_1^2 \mathrm{e}^{2\mathrm{M}} + D_2^2 \mathrm{e}^{-2\mathrm{M}} - (D_1^2 + D_2^2)\cos\tau]\right\} \tag{23}$$

Equation (22) along with constants given by eq. (18) and eq. (23) completely defines the temperature field. Equation (22) gives:

$$\frac{\mathrm{d}\theta}{\mathrm{d}y} = -\tau D_3 \sin(\tau y) + \tau D_4 \cos(\tau y) - \frac{4\mathrm{BrM}^3 N_1}{4\mathrm{M}^2 + QN_1}(D_1^2 \mathrm{e}^{2\mathrm{M}y} - D_2^2 \mathrm{e}^{-2\mathrm{M}y}) \tag{24}$$

The critical Brinkman number (CBr) is that value of Brinkman number at which heat transfer changes its direction, hence consequently CBr is obtained by equating $\mathrm{d}\theta/\mathrm{d}y = 0$. The expression for CBr at the upper moving plate ($y = 1$) is obtained as:

$$\mathrm{CBr} = \frac{(4\mathrm{M}^2 + QN_1)}{2\mathrm{M}^2 N_1} \cdot$$

$$\cdot \frac{-\tau\cot\tau}{\left[D_1^2(-2\mathrm{Me}^{2\mathrm{M}} + \tau\mathrm{e}^{2\mathrm{M}}\cot\tau + \tau\operatorname{cosec}\tau) + D_2^2(2\mathrm{Me}^{-2\mathrm{M}} + \tau\mathrm{e}^{-2\mathrm{M}}\cot\tau + \tau\operatorname{cosec}\tau)\right]} \tag{25}$$

Case II – Adiabatic – isothermal walls

This case deals with the situation where lower wall is at uniform temperature T_0 and at the upper wall, $\partial T/\partial y = 0$. In this case the energy eq. (7) in non-dimensional form after dropping asterisks and using eqs. (2) and (19) becomes:

$$\frac{\mathrm{d}^2\theta}{\mathrm{d}y^2} + \frac{Q}{1 + \frac{4N}{3}}\theta = \frac{-\mathrm{Br}}{1 + \frac{4N}{3}}\left[\left(\frac{\mathrm{d}u}{\mathrm{d}y}\right)^2 + \mathrm{M}^2 u^2\right] \tag{26}$$

where $N = 4\sigma_1 T_0^3/k_1\kappa$, $\mathrm{Br} = \mu u_1^2/\kappa T_0$, and $Q = Q_0 h^2/\kappa$ are the radiation parameter, Brinkman number, and heat source parameter, respectively. On using eq. (16), eq. (26) takes the following form:

$$\frac{\mathrm{d}^2\theta}{\mathrm{d}y^2} + \frac{Q}{1 + \frac{4N}{3}}\theta = \frac{-2\mathrm{BrM}^2}{1 + \frac{4N}{3}}(D_1^2 \mathrm{e}^{2\mathrm{M}y} + D_2^2 \mathrm{e}^{-2\mathrm{M}y}) \tag{27}$$

Solving eq. (27), we get the temperature:

$$\theta = D_5 \cos \tau y + D_6 \sin \tau y - \frac{2\mathrm{BrM}^2 N_1}{4\mathrm{M}^2 + QN_1}(D_1^2 \mathrm{e}^{2\mathrm{M}y} + D_2^2 \mathrm{e}^{-2\mathrm{M}y}) \quad (28)$$

where D_5 and D_6 are constants of integration.

On applying boundary conditions (17) (for case II) to eq. (28) the constants D_5, and D_6 are obtained as:

$$D_5 = \frac{2\mathrm{BrM}^2 N_1 (D_1^2 + D_2^2)}{4\mathrm{M}^2 + QN_1}$$

$$D_6 = \frac{2\mathrm{BrM}^2 N_1}{(\tau \cos\tau)(4\mathrm{M}^2 + QN_1)}\left[D_1^2(\tau \sin\tau + 2\mathrm{Me}^{2\mathrm{M}}) + D_2^2(\tau \sin\tau - 2\mathrm{Me}^{-2\mathrm{M}})\right] \quad (29)$$

Equation (28) along with constants given by eqs. (18) and (29) completely defines the temperature field when there is no heat flux through the upper wall and lower wall is at uniform temperature.

Results and discussions

The effects of the various parameters on the momentum and the thermal regimes have been depicted through graphs and tables. The rate of heat transfer at walls and the critical Brinkman number have also been determined.

The effects of various parameters on the fluid velocity have been shown in fig. 2. The effect of various parameters on temperature field is shown in figs. 3(a), 4(a), and 5(a) (for case I) and figs. 3(b), 4(b) and 5(b) (for case II). The variation in the rate of heat transfer with respect to different parameters is shown in figs. 6(a)-9(a) (for case I), and figs. 6(b)-9(b) (for case II).

Figure 2 indicates that as the permeability parameter k increases, the velocity registers increments wherein it should be noted that the naturally permeable bottom has low values for k. This manifests the pertinent findings that a porous lining with even small permeability may be crucial. The effect of low permeability on the thermal regime is also interesting to observe as would follow in the coming analysis.

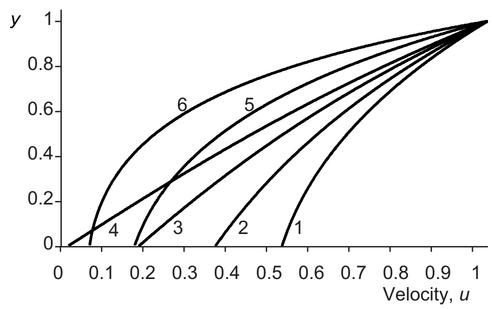

Figure 2. Velocity profiles for variation in M and k where line 1 – M = 1, k = 0.1, line 2 – M = 1, k = 0.01, line 3 – M = 1, k = 0.001, line 4 – M = 1, $k \cong 0$, line 5 – M = 2, k = 0.01, line 6 – M = 3, and k = 0.01; wehen N = 1, Q = 1, α = 0.1, and Br = 50

Figure 2 also shows that on increasing the Hartmann number and keeping the other parameters fixed we find that the fluid velocity decreases. This goes well with the expectations since the applied Lorentz force is transverse to the fluid flow direction hence consequently has an opposing effect on the flow velocity. This retardation produces quantitative and qualitative effect on the thermal regime too when Joule dissipation is taken into account.

The effects of permeability k and Hartmann number on the temperature is shown in fig. 3(a) for the case I and in fig. 3(b) for the case II. Both these figures show that with the increasing values of the Hartmann number the temperature of the fluid increases while

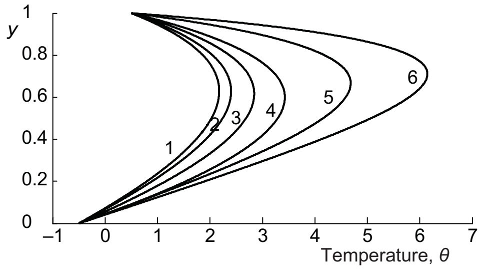

Figure 3(a). Temperature profiles (isothermal case) for variation in M & *k* where line 1 – M = 1, *k* = 0.1, line 2 – M = 1, *k* = 0.01, line 3 – M = 1, *k* = 0.001, line 4 – M = 1, *k* ≅ 0, line 5 – M = 2, *k* = 0.01, line 6 – M = 3, and *k* = 0.01; when *N* = 1, *Q* = 1, *α* = 0.1, and Br = 50

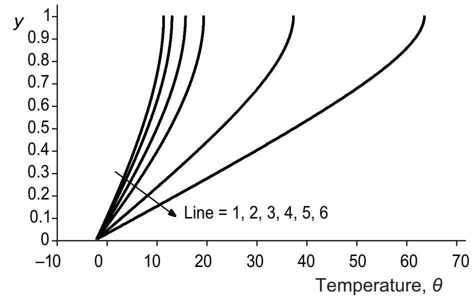

Figure 3(b). Temperature profiles (no flux case) for variation in M & *k* where line 1 – M = 1, *k* = 0.1, line 2 – M = 1, *k* = 0.01, line 3 – M = 1, *k* = 0.001, line 4 – M = 1, *k* ≅ 0, line 5 – M = 2, *k* = 0.01, line 6 – M = 3, and *k* = 0.01; when *N* = 1, *Q* = 1, *α* = 0.1, and Br = 50

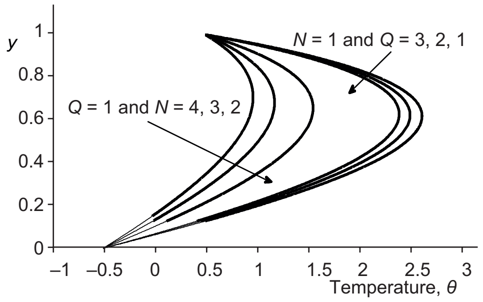

Figure 4(a). Temperature profiles (isothermal case): for variable *N* and *Q* when M = 1, *k* = 0.01, *α* = 0.1, and Br = 50

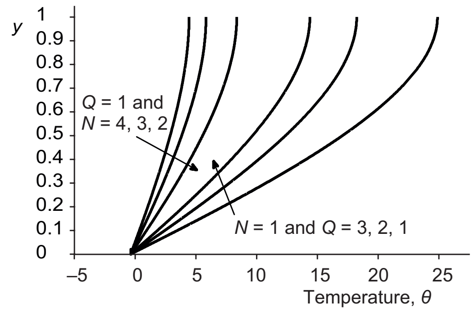

Figure 4(b). Temperature profiles (no flux case): for variable *N* and *Q* when M = 1, *k* = 0.01, *α* = 0.1, and Br = 50

increase in the permeability parameter k produces a decay in the fluid temperature. The effect of magnetic field can be understood if we have a look at the energy equation. The term which accounts for Joule dissipation in fact serves as a heat source and consequently contributes to rise in the temperature.

The variation of temperature with the radiation parameter N and heat source parameter Q is shown in fig. 4(a) for the case I and in fig. 4(b) for the case II. Both the figures show that there is an increase in temperature with the increase in Q whereas it decreases with the increasing values of N.

We now have a look on the variation in the rate of heat transfer for case I, figs. 6(a)-9(a).

Figure 6(a) clearly indicates that as the permeability parameter k decreases, the rate of heat transfer at the upper wall decreases and whereas, it increases at the lower wall. Figure 7(a) exhibits that with the increase in Hartmann number, the rate of heat transfer at the upper wall decreases whereas at the lower wall it increases. Figure 8(a) indicates that with the increase in radiation parameter N the rate of heat transfer at the upper wall increases whereas at the lower wall it decreases. It is clear from fig. 9(a) that as the heat source parameter Q increases the rate of heat transfer at the upper wall decays whereas at the lower wall it increases.

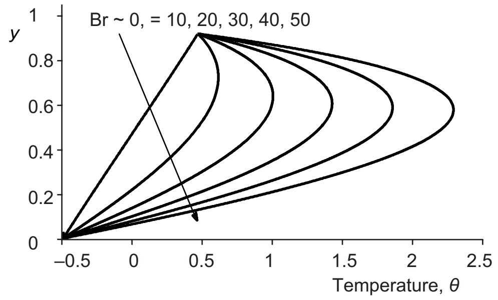

Figure 5(a). Temperature profiles (isothermal case): for variable Br when M = 1, *k* = 0.01, *α* = 0.1, *N* = 1, and *Q* = 1

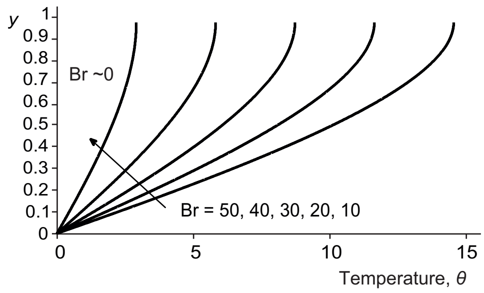

Figure 5(b). Temperature profiles (no flux case): for variable Br when M = 1, *k* = 0.01, *α* = 0.1, *N* = 1, and *Q* = 1

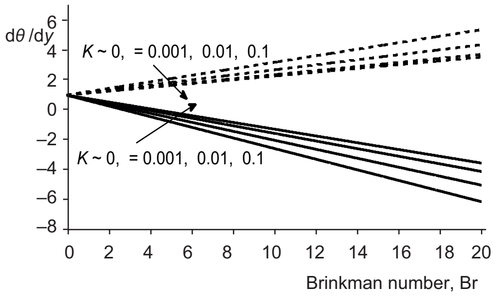

Figure 6(a). Rate of heat transfer (case I): at *y* = 1 (solid) and *y* = 0 (dotted) for variable *k* when M = 1, *N* = 1, *α* = 0.1, and *Q* = 1

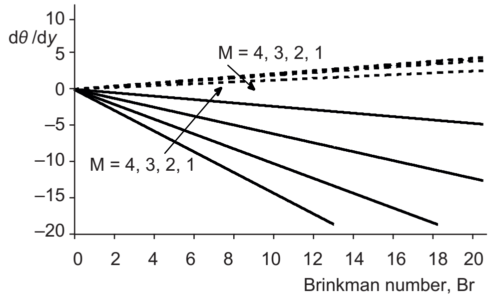

Figure 7(a). Rate of heat transfer (case II): at *y* = 1 (solid) and *y* = 0 (dotted) for variable M when *k* = 0.01, *N* = 1, *α* = 0.1, and *Q* = 1

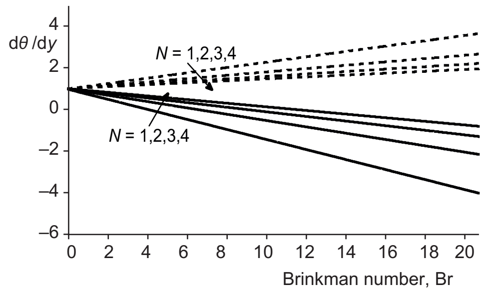

Figure 8(a). Rate of heat transfer (case I): at *y* = 1 (solid) and *y* = 0 (dotted) for variable *N*, when M = 1, *Q* = 1, *α* = 0.1, and *k* = 0.01

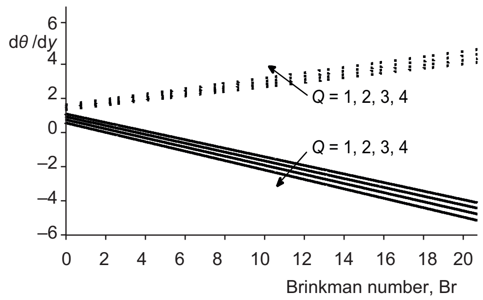

Figure 9(a). Rate of heat transfer (case II): at *y* = 1 (solid) and *y* = 0 (dotted) for variable *Q* when M = 1, *N* = 1, *α* = 0.1, and *k* = 0.01

We now analyze the variation in the rate of heat transfer for the case II, figs. 6(b)-9(b). In this case there is no heat transfer from the upper impermeable moving wall. The rate of heat transfer at the lower naturally permeable boundary is discussed. Figure 6(b) clearly indicates that as the permeability parameter *k* decreases, the rate of heat transfer at the lower wall increases. Figure 7(b) unequivocally says that as the Hartmann number M increases the rate of heat transfer increases at the lower wall. Figure 8(b) indicates that with the increase in radiation parameter N the rate of heat transfer at the lower boundary decreases. It is clear from fig. 9(b) that as the heat source parameter Q increases, the rate of heat transfer increases at the lower permeable boundary.

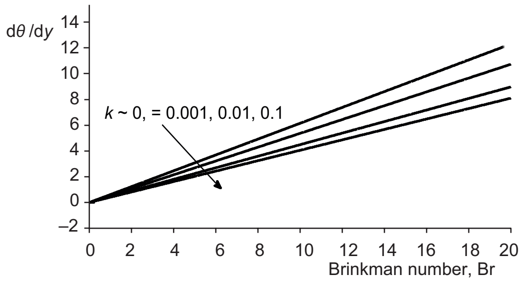

Figure 6(b). Rate of heat transfer (no flux case) at the lower naturally permeable boundary (y = 0) for varying values of k when M = 1, N = 1, α = 0.1, and Q = 1

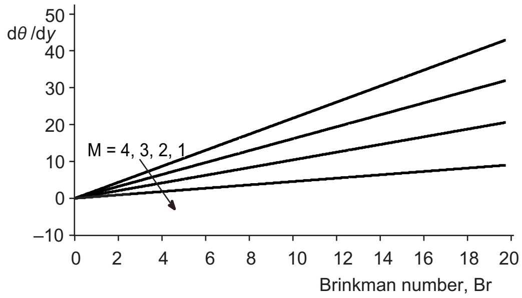

Figure 7(b). Rate of heat transfer (no flux case) at the lower naturally permeable boundary (y = 0) for varying values of M when k = 0.01, N = 1, α = 0.1, and Q = 1

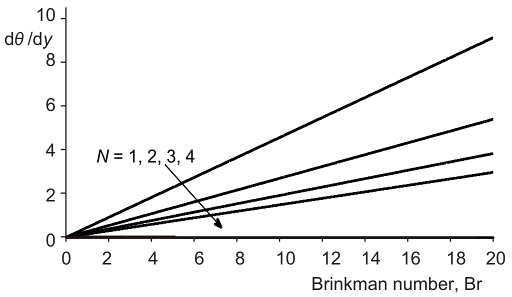

Figure 8(b). Rate of heat transfer (no flux case) at the lower naturally permeable boundary (y = 0) when N varies when k = 0.01, M = 1, α = 0.1, and Q = 1

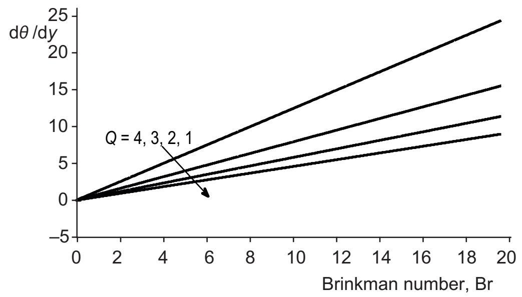

Figure 9(b). Rate of heat transfer (no flux case) at the lower naturally permeable boundary (y = 0) when Q varies when k = 0.01, N = 1, α = 0.1, and M = 1

Critical Brinkman number is that value of Brinkman number at which the heat transfer changes its direction. The variation of critical Brinkman number (CBr1) at the upper wall (y = 1) for case I (isothermal case) with respect to various parameters is shown in tabs. 1-2.

Table 1 shows the effects of various parameters on CBr. When M = 0 = N = Q = k then CBr comes out to be 2.0402. Here $k \to 0$ corresponds to impermeable bottom. When permeable boundary is introduced, and k = 0.01, M = 0 = Q = N then CBr attains the value 8. The effect of Lorentz force is to decrease CBr as we see that when M = 1 and other parameters are zero, CBr reduces to 1.2324 as compared to its value 2.0402 when all parameters are zero. From this table it is also clear that the introduction of radiation enhances the CBr value while the introduction of heat source parameter Q causes decay in CBr.

Tables 2 and 3 display the values of CBr for numerous cases of varying values of the parameters. Table 2 displays the variation in CBr with respect to M and N when k = 0.01, Q = 1 The table shows that when M = 0 and N = 1, CBr = 15.3479 but as soon as the magnetic field is introduced with strength M = 1, CBr dips drastically to 3.4090 and decreases further with increasing values of M. When N = 0 and other parameters are non-zero CBr = 1.0570 but as radiation is introduced with strength N = 1, CBr increases to 3.4090 which further increases with the increasing values of k. Table 3 displays the effect of permeability parameter k and heat source Q on CBr. It is evident from the table that as Q increases CBr decreases while CBr increases with the increasing values of k.

Table 1. Variation in CBr (isothermal case)

M	N	Q	k	CBr
0	0	0	0	2.0402
0	0	0	0.01	8.0000
1	0	0	0	1.2324
0	1	0	0	4.7605
0	0	1	0	1.1828

Table 2. Variation in CBr (isothermal case) with M and *N* when *k* = 0.01, and *Q* = 1

M	N	CBr
0	1	15.3479
1	1	3.4090
2	1	1.3055
3	1	0.7839
4	1	0.5608
1	0	1.0570
1	2	5.7587
1	3	8.1079
1	4	10.4569

Table 3. Variation in CBr (isothermal case) with M and *N* when M = 1, and *N* = 1

K	Q	CBr
0	1	2.3983
0.001	1	2.8093
0.01	1	3.4090
0.1	1	3.8306
0.2	1	3.9062
0.01	0	4.1104
0.01	2	2.7028
0.01	3	1.9913
0.01	4	1.2744

Conclusions

The main objective of the present work is to investigate the effects of permeable boundary on the radiative heat transfer with dissipative effects relative to the heat flow resulting from the impressed temperature difference of the channel walls. On the basis of this study we may conclude following:

- The naturally permeable boundary has a significant impact on the momentum and thermal regime.
- As the strength of the magnetic field increases the effect of permeability on the fluid velocity, fluid temperature, rate of heat transfer and critical Brinkman number becomes insignificant and the fluid flows within the channel as if no permeable boundary is present.
- Increased magnetic field parameter retards the flow. As we increase the permeability parameter the velocity of the fluid increases.
- For both cases (I and II) when the upper wall is isothermal/adiabatic we infer:
  – On increasing the permeability parameter both the fluid temperature and $\theta'(0)$ decrease.
  – On increasing the Hartmann number both the fluid temperature and $\theta'(0)$ increase.
  – With the increase in radiation parameter both the temperature and $\theta'(0)$ decrease.
  – With the increase in source parameter both the temperature and $\theta'(0)$ increase.
  – As we increase the Brinkman number a rise in the fluid temperature is observed.
- For case I, when the channel walls are isothermal we infer that:

– On increasing the permeability and radiation parameter both $\theta'(1)$ and CBr increase.
– On increasing Hartmann number and heat source parameter $\theta'(1)$ and CBr, both decrease.
– With the increase in heat source parameter, both $\theta'(1)$ and CBr decrease.

Nomenclature

B – constant, [–]
B_0 – uniform transverse magnetic field, [T]
Br – Brinkman number
Case I = $\mu(u_1)^2/\kappa(T_1 - T_0)$, and
Case II = $\mu(u_1)^2/(\kappa T_0)$, [–]
g – gravitational acceleration, [ms^{-2}]
h – channel width, [m]
k – permeability, [m^2]
k* – dimensionless permeability, [–]
k_1 – mean absorption coefficient, [m^{-1}]
M – Hartmann number [= $(\sigma B_0{}^2h^2/\mu)^{-1/2}$], [–]
N – radiation parameter
{ = $[4\sigma_1(T_m)^3]/(k_1\kappa)$}, [–]
p – fluid pressure, [kg m^{-1}s^{-2}]
p_0 – constant pressure at origin, [kg m^{-1}s^{-2}]
Q – heat source parameter (= Q_0h^2/κ), [–]
Q_0 – uniform heat source
q_r – radiation heat flux
[= $(-4\sigma_1/3k_1)(\partial T^4/\partial y)$], [kgm^{-2}]
T – fluid temperature, [K]
T_0 – temperature of lower permeable boundary, [K]
T_1 – temperature of upper wall for case I, [K]
u, v, w – velocity components along x-, y-, and z- directions, respectively, [ms^{-1}]
u^*, v^*, w^* – dimensionless velocity components, [–]
u_1 – velocity of upper wall, [ms^{-1}]
x – Cartesian co-ordinate along the permeable boundary, [m]
x^*, y^*, z^* – dimensionless Cartesian co-ordinates, [–]
y – Cartesian co-ordinate along the width of the channel, [m]
z – Cartesian co-ordinate normal to the channel, [m]

Greek symbols

α – empirical constant, [–]
θ – dimensionless fluid temperature, [K]
μ – dynamic viscosity, [Nsm^{-2}]
κ – thermal conductivity, [kgms^{-3}K^{-1}]
ρ – fluid density, [kgm^{-3}]
σ – electrical conductivity, [Sm^{-1}]
σ_1 – Stefan Boltzmann constant, [kgm^{-2}K^{-4}]

References

[1] Leadon, B. M., Plane Couette Flow of a Conducting Gas through a Transverse Magnetic Field, Convair Scientific Research Laboratory, San Diego, Cal., USA, Research note No. 13, 1957
[2] Verma, P. D., Bhatt, B. S., Plane Couette Flow of Two Immiscible Incompressible Fluids with Uniform Suction at the Stationary Plate, *Proceedings Mathematical Science*, *78* (1973), 3, pp. 108-120
[3] Chauhan, D. S., Vyas, P., Heat Transfer in Hydromagnetic Couette flow of Compressible Newtonian Fluid, *ASCE Journal of Engineering Mechanics*, *121* (1995), 1, pp. 57-61
[4] Kuznetsov, A. V., Analytical Investigation of Couette Flow in a Composite Channel Partially Filled with a Porous Medium and Partially with a Clear Fluid, *Int. J. of Heat Mass Transfer*, *41* (1998), 16, pp. 2556-2560
[5] Chauhan, D. S., Kumar, V., Heat Transfer Effects in a Couette Flow through a Composite Channel Partially Filled by a Porous Medium with a Transverse Sinusoidal Injection Velocity and Heat Source, *Thermal Science*, *15* (2011), Suppl. 2, pp. S175-S186
[6] Berman, A. S., Laminar Flow in Channels with Porous Walls, *J. Appl. Phys.*, *24* (1953), 9, pp. 1232-1235
[7] Beavers, G. S., Joseph, D. D., Boundary Conditions at a Naturally Permeable Wall, *J. Fluid Mech.*, *30* (1967), 1, pp. 197-207
[8] Taylor, G. I., A Model for the Boundary Condition of a Porous Material, Part 1, *J. Fluid Mech.*, *49* (1971), 2, pp. 319-326
[9] Richardson, S., A Model for the Boundary Condition of a Porous Material, Part 2, *J. Fluid Mech.*, *49* (1971), 2, pp. 327-336
[10] Larson, R. E., Higdon, J. J. L., Microscopic Flow Near the Surface of Two Dimensional Porous Media, Part 2, Transverse flow, *J. Fluid Mech.*, *178* (1987), 1, pp. 119-136

[11] Sahraoui, M., Kaviany, M., Slip and no-Slip Velocity Boundary Conditions at the Interface of Porous Plain Media, *Int. J. Heat Mass Transfer*, *35* (1992), 4, pp. 927-943
[12] Vafai, K., Kim, S. J., Fluid Mechanics of the Interface Region between a Porous Medium and a Fluid Layer – An exact solution, *Int. J. Heat Fluid Flow*, *11* (1990), 3, pp. 254-256
[13] Klikenberg, L. J., The Permeability of Porous Media to Liquids and Gases, *Drilling and Production Practices*, American Petroleum Institute, Washington, DC., USA, 1941, pp. 200-213
[14] Saffman, P. G., On the Boundary Condition at the Surface of a Porous Medium, *Studies in Applied Mathematics*, L (1971), 2, pp. 93-101
[15] Makinde, O. D., Osalusi, E., MHD Steady Flow in a Channel with Slip at the Permeable Boundaries, *Rom. Journ. Phys.*, *51* (2006), 3-4, pp. 319-328
[16] Singh, R. K., *et al*., On Hydromagnetic free Convection in the Presence of Induced Magnetic Field, *Heat and Mass Transfer*, *46* (2010), 5, pp. 523-529
[17] Nikodijevic, D., *et al*., MHD Couette Two-Fluid Flow and Heat Transfer in Presence of Uniform Inclined Field, *Heat and Mass Transfer*, *47* (2011), 12, pp. 1525-1535
[18] Viskanta, R., Heat Transfer in a Radiating Fluid with Slug Flow in a Parallel Plate Channel, *Applied Scientific Research*, *13* (1964), 1, pp. 291-311
[19] Helliwell, J. B., On the Stability of Thermally Radiative Magnetofluiddynamic Channel Flow, *Journal of Engineering Mathematics*, *11* (1977), 1, pp. 67-80
[20] Elsayed, M. M., Fathalah, K. A., Simultaneous Convection and Radiation in Flow between Two Parallel Plates, *Int. J. of Heat and Fluid Flow*, *3* (1982), 4, pp. 207-212
[21] Helliwell, J. B., Mosa, M. F., Radiative Heat Transfer in Horizontal Magnetohydrodynamic Channel Flow with Buoyancy Effects and an Axial Temperature Gradient, *Int. J. Heat Mass Transfer*, *22* (1979), 5, pp. 657-668
[22] Elbashbeshy, E. M. A., Emam, T. G., Effects of Thermal Radiation and Heat Transfer over an Unsteady Stretching Surface Embedded in a Porous Medium in the Presence of Heat Source or Sink, *Thermal Science*, *15* (2011), 2, pp. 477-485
[23] Gebhart, B., Effect of Viscous Dissipation in Natural Convection, *J. Fluid Mech., 38* (1962), 2, pp. 225-232
[24] Gebhart, B., Mollendorf, J., Viscous Dissipation in External Natural Convection Flows, *J. Fluid Mech., 38*(1969), 1, pp. 97-107
[25] Magyari, E., Keller, B., The Opposing Effects of Viscous Dissipation Allows for a Parallel Free Convection Boundary-Layer Flow along a Cold Vertical Flat Plate, *Transp. Porous Media, 51* (2003), 2, pp. 227-230
[26] Rees, D. A. S., *et al*., The Development of the Asymptotic Viscous Dissipation Profile in a Vertical Free Convective Boundary Layer Flow in a Porous Medium, *Transp. Porous Media, 53* (2003), 3, pp. 227-230
[27] Illingworth, C. R., Some Solutions of the Equations of Flow of a Viscous Compressible Fluid, *Proc. Cambr. Phil. Soc.*, *46* (1950), 3, pp. 469-478
[28] Morgan, A. J. A., On the Couette Flow of a Compressible Viscous, Heat Conducting, Perfect Gas, *JAS*, *24* (1957), April, pp. 315-316
[29] Modest, M. F., *Radiative Heat Transfer*, 2nd ed., Academic Press, New-York, USA, 2003

Paper submitted: August 28, 2012
Paper revised: July 8, 2013
Paper accepted: July 16, 2013